energies

MDPI

Article

Ferrocene Derivatives Functionalized with Donor/Acceptor (Hetero)Aromatic Substituents: Tuning of Redox Properties

Norberto Manfredi *, Cristina Decavoli, Chiara L. Boldrini, Carmine Coluccini and Alessandro Abbotto *

Department of Materials Science and Solar Energy Research Centre MIB-SOLAR, University of Milano-Bicocca, and INSTM Milano-Bicocca Research Unit, Via Cozzi 55, 20125 Milan, Italy; c.decavoli@campus.unimib.it (C.D.); chiara.boldrini@unimib.it (C.L.B.); carmine.coluccini@unimib.it (C.C.)

* Correspondence: norberto.manfredi@unimib.it (N.M.); alessandro.abbotto@unimib.it (A.A.)

Received: 26 June 2020; Accepted: 21 July 2020; Published: 1 August 2020

Abstract: A series of functionalized ferrocene derivatives carrying electron-donor and electron-withdrawing (hetero)aromatic substituents has been designed as potential alternative electrolyte redox couples for dye-sensitized solar cells (DSSC). The compounds have been synthesized and fully characterized in their optical and electrochemical properties. A general synthetic approach that implies the use of a microwave assisted Suzuki coupling has been developed to access a significative number of compounds. The presence of different electron-rich and electron-poor substituents provided fine tuning of optical properties and energy levels. HOMO and LUMO energy values showed that the substitution of one or two cyclopentadienyl rings of ferrocene can be successfully exploited to increase the maximum attainable voltage from a standard DSSC device using TiO_2 as a semiconductor, opening the way to highly efficient, non-toxic, and cheap redox shuttles to be employed in solar energy technologies.

Keywords: ferrocene; dye-sensitized solar cells; iodine-free electrolyte

1. Introduction

Over the past two decades, hybrid organic-inorganic solar cells, in particular dye-sensitized solar cells (DSSC), have attracted a huge interest in the scientific community. Since their first report by Graetzel in 1991 [1], DSSC have continuously increased their power conversion efficiencies (PCE), recently reaching a record efficiency exceeding 14% [2–7]. A DSSC is a multi-component device comprising: (a) a dye-sensitizer (in general, a Ru(II) complex or a polar donor-acceptor organic chromophore); (b) a n-type semiconductor metal oxide (consisting of one or more mesoporous layers of TiO_2); (c) a redox electrolyte (typically the iodide/triiodide couple, I^-/I_3^-, redox pair); (d) a transparent working anode and a counter electrode (based on fluorine-doped tin oxide, FTO). These devices are unique in terms of their parameter's optimization since the investigation on their different chemical component makes possible to finely tune any single electrical parameters of the device, thus separately optimizing the open circuit photovoltage V_{oc} or the short-circuit photocurrent J_{sc}.

In a DSSC the open-circuit photovoltage, to which the PCE is directly related following the relationship PCE = $V_{oc} \times J_{sc} \times$ FF (FF = fill factor), is proportional to the saturation current of the cell, in turn depending on the energy difference between the TiO_2 quasi-Fermi level and the redox potential of the redox couple electrolyte [8]. The iodide/triiodide couple (0.35 V vs. NHE) is the most common electrolyte in DSSC, affording record power conversion efficiencies [9]. Unfortunately, it suffers some serious limitations, mainly corrosion of metals in devices and complex redox chemistry. In particular,

a large overpotential is needed for efficient dye regeneration owing to the formation of an intermediate radical species I_2 (0.93 V). This aspect automatically limits the maximum achievable V_{oc} to values significantly lower than 1 V [10,11]. Thus, in order to enhance the photovoltage and minimize the dye regeneration overpotential, new redox shuttles with lower redox levels are needed, while keeping the energy offset with the dye HOMO level required for efficient dye regeneration (>0.2–0.3 V) [11].

A variety of iodide/triiodide-free electrolytes have been so far proposed for liquid DSSC [12–18]. Among others, Co-polypyridyl complexes with more positive potentials vs. NHE have been proposed [12] and investigated in the past decade, recently achieving excellent performances [19–24] and high PCEs [6]. In Co-based device, an increase of the photovoltage and photocurrent compared to the iodide /triiodide redox couple has been observed [20]. The nature of the ligands of the complexes determines the potential of the electrolyte. A drawback associated to a more positive potential is the faster recombination rate with the electrons injected on the titanium dioxide. A way to limit this resides in the proper design of the dye. The choice of a sensitizer with hydrophobic chains resulted the key to improve the cell performances [20,25–28]. A record efficiency was reached by using a porphyrin dye and a Co-polypyridyl electrolyte [6]. Unfortunately, Co-polypyridyl complexes are not always readily available and their market application may be hampered by their high cost and, in some cases, toxicity [19].

Apart from Co(II)/Co(III) complexes, other reported iodide/triiodide-free electrolytes always afforded lower efficiencies [29]. Up to now, the best efficiency of alternative redox shuttles, 7.5%, has been achieved by the ferrocene/ferrocenium (Fc/Fc^+) redox couple under 1 sun (1000 W m^{-2}) irradiation [10]. Iron is a very abundant, cheap, and non-toxic metal. Its most common complex, ferrocene (Fc), undergoes a simple monoelectronic redox chemistry affording its oxidized derivative ferrocenium Fc^+, with a potential of +0.63 V vs. NHE [10,11], that is ~+0.3 V more positive than the iodide/triiodide couple. Because of these unique and convenient features, the Fc/Fc^+ redox couple is thus highly attractive as an electrolyte in DSSC.

The presence of electron-donating (donor, D) and electron-withdrawing (acceptor, A) substituent effects might represent an efficient way to finely tune the redox energy levels of Fc derivatives. Moreover, shifting the potential of the redox couple to more positive values provides a straightforward strategy to significantly increase the cell photovoltage compared to iodine-based DSSC. Spiccia and co-workers [30] investigated mono- and bis-bromoferrocene derivatives (in the latter the two bromines were located on different cyclopentadienyl rings) and several alkylated ferrocenes. The redox potentials of the brominated compounds were more positive (0.78 V and 0.83 V vs. NHE for the mono- and the bis-bromoferrocene, respectively) than those of unsubstituted or alkyl-substituted ferrocenes [11]. Hupp and co-workers [31] have investigated mono- and bis-chloroferrocene, with the two chlorine atoms located on different cyclopentadienyl rings. Very interestingly, the redox potential of the corresponding Fc/Fc^+ couples were calculated as 0.81 V and 0.94 V vs. NHE, respectively, affording an additional gain of ~0.3 V compared to the pristine Fc/Fc^+ pair, and of ~0.6 V compared to I^-/I_3^-. Dimethylferrocene was also tested as an electrolyte in DSSC in combination with boron-dipyrromethene (BODIPY)-based dyes as sensitizers [32]. More recently, Fc derivatives and different complexes of Fe have been used as redox shuttles in n- and p-type DSSC with interesting efficiencies highlighting the possibility of using Fe derivatives as electrolytes also in tandem n-type/p-type DSSC [32,33].

While searching for Fc derivatives with appropriate redox potential to be employed as DSSC electrolytes, we were surprised to find that not only Fc derivatives substituted with aromatic and heteroaromatic groups have been ever used as electrolytes in DSSC, but even in the whole Fc literature such derivatives have been very scantly investigated. This attracted our attention since it is well-known that aromatic and heteroaromatic D and A substituents can greatly affect the redox properties of the main scaffold to which they are bound. In particular, D and A groups are expected to decrease and increase the oxidation potential, respectively. In other terms, aromatic and heteroaromatic D and A substituents of Fc are expected to shift the redox potential to either less or more positive values vs. NHE compared to the reference Fc/Fc^+ couple.

In this paper we describe a series of Fc/Fc^+ redox derivatives, where the Fc core is substituted by one or two (located on different cyclopentadienyl rings) representative aromatic and heteroaromatic D and A substituents. The new mono- and bis-D- and A-substituted Fc/Fc^+ have been investigated in their synthetic access, spectroscopic, and electrochemical properties, as a function of the electronic properties of the inserted substituent(s). Finally, spectroelectrochemical investigation has been carried out to evaluate the optical properties of the oxidized form Fc^+ and asses the reversibility of the redox process in order to support the potential use of the substituted new Fc/Fc^+ redox shuttles as alternative cheap and efficient DSSC electrolytes.

2. Materials and Methods

2.1. General Information

1-bromo-2,4-dihexyloxybenzene was synthesized following a procedure previously reported in literature [34]. Commercially available reagents were purchased at the highest purity grade and used without any further purification. Purification of the synthesized compounds via flash chromatography has been performed with silica gel 230–400 mesh (60 Å). The reactions performed under nitrogen atmosphere have been conducted in oven-dried glassware and monitored by thin-layer chromatography by using UV light (254 and 365 nm) as a visualizing agent. Anhydrous solvents were purchased from commercial suppliers and used as received. After extraction, the organic phases have been dried with anhydrous Na_2SO_4 and filtered before evaporation of the solvents at reduced pressure. Absorption spectra were recorded with a V-570 Jasco spectrophotometer. A Bruker AMX-500 spectrometer operating at 500.13 MHz (^1H) and 125.77 MHz (^{13}C) was used. High resolution mass spectra have been recorded with an Agilent 6230B Time of Flight (TOF) equipped with an electrospray (Dual ESI) source.

Cyclic voltammetry (CV) have been performed in 0.1 M $TBAClO_4$ in MeCN supporting electrolyte at 100 mV s^{-1} scan rate, with an AUTOLAB PGSTAT302N potentiostat in a three-electrode electrochemical cell under an Ar flow. The working, counter, and the pseudo-reference electrodes were a gold pin for the dyes in solution, a Pt wire, and an Ag/AgCl electrode (3 M KCl), respectively. Before measurements, the Pt wire was cleaned in an ultrasonic bath for 15 min in deionized water, rinsed with 2-propanol, and cycled for 50 times in 0.5 M H_2SO_4. The Ag/AgCl pseudo-reference electrode has been calibrated, by adding Fc (10^{-3} M) to the test solution after each measurement. The spectroelectrochemical measurements have been carried out using the same cell arrangement in a sealed optical cuvette. A Jasco V-570 UV-Vis-near IR was used as spectrophotometer in the visible (Vis) spectra ($800 > \lambda > 400$ nm) under several applied potentials. The potential was applied before the spectrum acquisition for a time long enough to drive the system to a stationary state, and it was maintained during the measurements.

2.2. Synthesis of Fc Derivatives

General procedure A for mono-substituted Fc derivatives: A mixture of ferroceneboronic acid (1.2 mmol), arylbromide (1.0 mmol), $Pd(dppf)Cl_2{\cdot}CH_2Cl_2$ (0.02 mmol), an aqueous solution 1 M of Bu_4NOH (1.6 mmol), 1,4-dioxane (5 mL) was stirred in a microwave reactor (130 °C, 200 psi, 90 W) for 4 h. As an alternative method, the mixture could be stirred at reflux for 24 h under inert and conventional (not microwave) conditions. H_2O was added and the solution was extracted with CH_2Cl_2. The organic layers were dried with Na_2SO_4. Flash chromatography was finally applied to obtain the pure product.

4-ferrocenylpyridine and 1,1′-bis(4-pyridyl)ferrocene (**1a**,**1b**). A mixture of 1,1′-ferrocenediboronic acid bis(pinacol) ester (658 mg, 1.50 mmol), 4-bromopyridine hydrochloride (733 mg, 3.78 mmol), $Pd(dppf)_2Cl_2{\cdot}CH_2Cl_2$ (26 mg, 0.03 mmol), 1,4-dioxane (7.5 mL), an aqueous solution 1 M of Bu_4NOH (7.5 mL, 7.5 mmol) was stirred in a microwave reactor (130 °C, 200 psi, 90 W) for 4 h. H_2O was added and the solution was extracted with CH_2Cl_2. The organic layers were dried with Na_2SO_4. Flash chromatography afforded the pure products (CH_2Cl_2/MeOH 97/3 for the mono-4-ferrocenylpyridine and 80/20 for the bis-4-ferrocenylpyridine). 4-ferrocenylpyridine **1a**,

(80 mg, 20%). ^{1}H NMR (500 MHz, $CDCl_3$) δ(ppm) = 8.46 (s, 2H), 7.31 (s, 2H), 4.70 (s, 2H), 4.40 (s, 2H), 4.02 (s, 5H). ^{13}C NMR (125 MHz, $CDCl_3$) δ(ppm) = 149.69, 148.56, 120.57, 80.93, 70.21, 69.96, 66.83. 1,1′-bis(4-pyridyl)ferrocene **1b** (96 mg, 19%) ^{1}H NMR (500 MHz, $CDCl_3$) δ(ppm) = 8.39 (4H, s), 7.07 (4H, s), 4.44 (8H, d, *J* = 104.1 Hz). ^{13}C NMR (125 MHz, $CDCl_3$) δ(ppm) = 150.66, 147.37, 121.07, 72.73, 69.37.

5-hexyl-2-ferrocenylthiophene (**1c**). This product was synthesized according to the general procedure **A**: ferroceneboronic acid (689 mg, 3.01 mmol), 2-bromo-5-hexylthiophene (570 mg, 2.31 mmol), $Pd(dppf)Cl_2{\cdot}CH_2Cl_2$ (50 mg, 0.06 mmol), an aqueous solution 1 M of Bu_4NOH (3.8 mL, 3.80 mmol), 1,4-dioxane (13 mL). Flash chromatography (cyclohexane/ethyl acetate 95/5) afforded the pure product as an orange oil (469 mg, 44%). ^{1}H NMR (500 MHz, $CDCl_3$) δ(ppm) = 6.81 (d, *J* = 3.6 Hz, 1H), 6.59 (d, *J* = 3.2 Hz, 1H), 4.53 (s, 2H), 4.25 (s, 2H), 4.11 (s, 5H), 2.78 (t, *J* = 7.6 Hz, 2H), 1.71 (quintet, *J* = 7.6 Hz, 2H), 1.38 (m, 6H), 0.93 (t, *J* = 6.8 Hz, 3H). ^{13}C NMR (125 MHz, $CDCl_3$) δ(ppm) = 143.73, 140.19, 123.98, 121.89, 80.93, 69.87, 68.27, 66.69, 31.60, 31.52, 30.25, 28.82, 22.60, 14.09. HRMS (Dual-ESI) *m/z*: calcd. for $[M]^+$ $C_{20}H_{24}FeS$: 352.0948; found 352.0956.

5-ferrocenylthiophene-2-carboxaldehyde (**1d**). This product was synthesized according to the general procedure **A**: ferroceneboronic acid (200 mg, 0.87 mmol), 2-bromo-5-formylthiophene (250 mg, 1.31 mmol), $Pd(dppf)_2Cl_2{\cdot}CH_2Cl_2$ (70 mg, 0.09 mmol), an aqueous solution 1 M of Bu_4NOH (1.8 mL, 1.8 mmol), 1,4-dioxane (6 mL) were stirred and heated to 95 °C for 24 h under inert atmosphere. Flash chromatography (cyclohexane/CH_2Cl_2, 1/1) afforded the pure product as a red solid (116 mg, 45%). ^{1}H NMR (500 MHz, $CDCl_3$) δ(ppm) = 9.83 (s, 1H), 7.59 (d, *J* = 4.1 Hz, 1H), 7.08 (d, *J* = 4.1 Hz, 1H), 4.70–4.67 (m, 2H), 4.45–4.40 (m, 2H), 4.11 (m, 5H). ^{13}C NMR (125 MHz, $CDCl_3$) δ(ppm) = 182.38, 142.35, 137.54, 122.95, 113.18, 71.02, 70.47, 70.15, 67.71.

4-formylphenylferrocene (**1e**). This product was synthesized according to the general procedure **A**: ferroceneboronic acid (400 mg, 1.75 mmol), 2-bromobenzaldehyde (275 mg, 1.49 mmol), $Pd(dppf)Cl_2{\cdot}CH_2Cl_2$ (24 mg, 0.02 mmol), an aqueous solution 1 M of Bu_4NOH (2.0 mL, 2.00 mmol), 1,4-dioxane (10 mL). Flash chromatography (petroleum ether/ethyl acetate 9/1) afforded the pure product as red solid (198 mg, 39%). ^{1}H NMR (500 MHz, $CDCl_3$) δ(ppm) = 9.98 (s, 1H), 7.79 (dd, *J* = 8.2, 2.0 Hz, 2H), 7.60 (d, *J* = 8.3 Hz, 2H), 4.74 (s, 2H), 4.43 (s, 2H), 4.05 (s, 5H). ^{13}C NMR (125 MHz, $CDCl_3$) δ(ppm) = 191.65, 147.32, 134.04, 129.95, 126.11, 82.83, 70.15, 69.96, 67.06.

1,1′-bis(4-formylphenyl)ferrocene (**1f**). A mixture of 1,1′-ferrocenediboronic acid bis(pinacol) ester (270 mg, 0.62 mmol), 4-bromobenzaldehyde (226 mg, 1.22 mmol), $Pd(dppf)Cl_2{\cdot}CH_2Cl_2$ (51 mg, 0.06 mmol), an aqueous solution 1 M of Bu_4NOH (1.8 mL, 1.8 mmol), 1,4-dioxane (6 mL) was stirred in a microwave reactor (130 °C, 30 psi, 80 W) for 90 min. H_2O was added and the solution was extracted with CH_2Cl_2. The organic layers were dried with Na_2SO_4. Flash chromatography on silica gel (cyclohexane/CH_2Cl_2, from 9/1 to 7/3) was finally applied to obtain the pure product as a red solid (50 mg, 21%). ^{1}H NMR (500 MHz, $CDCl_3$) δ(ppm) = 9.92 (s, 2H), 7.62 (d, *J* = 8.1 Hz, 4H), 7.30 (d, *J* = 8.1 Hz, 4H), 4.61–4.59 (m, 4H), 4.38–4.36 (m, 4H). ^{13}C NMR (125 MHz, $CDCl_3$) δ(ppm) = 191.70, 144.81, 134.08, 129.86, 125.89, 84.17, 71.61, 68.46.

2,4-bis-hexyloxyphenylferrocene (**1g**). This product was synthesized according to general procedure **A**: ferroceneboronic acid (138 mg, 0.6 mmol), 1-bromo-2,4-bis-hexyloxybenzene (178 mg, 0.5 mmol), $Pd(dppf)_2Cl_2{\cdot}CH_2Cl_2$ (20 mg, 0.03 mmol), a solution 1 M of Bu_4NOH (0.6 mL, 0.6 mmol), 1,4-dioxane (6 mL) were stirred and heated to 95 °C for 24 h under inert atmosphere. Flash chromatography (cyclohexane/CH_2Cl_2 from 9/1 to 7/3) afforded the pure product as a reddish oil (70 mg, 30%). M.p. ^{1}H NMR (500 MHz, $CDCl_3$) δ(ppm) = 7.36 (d, *J* = 8.0 Hz, 1H), 6.44 (d, *J* = 1.7 Hz, 1H), 6.42 (m, 1H), 4.85 (m, 2H), 4.35 (m, 2H), 4.12 (s, 5H), 3.97 (m, 4H), 1.87 (m, 2H), 1.79 (m, 2H), 1.50 (m, 4H), 1.38 (m, 8H), 0,93 (m, 6H). ^{13}C NMR (125 MHz, $CDCl_3$) δ(ppm) = 158.7, 157.2, 129.5, 119.5, 105.1, 99.9, 85.1, 69.6, 68.3, 68.2, 68.1, 68.0, 31.6, 31.6, 29.4, 29.3, 25.9, 25.8, 22.6, 14.0. HRMS (Dual-ESI) *m/z*: calcd. for $[M]^+$ $C_{28}H_{38}FeO_2$: 462.2221; found 462.2223.

3. Results and Discussion

3.1. Design and Synthesis

The investigated mono- and bis-substitute Fc derivatives **1a–g** are listed in Figure 1. We have decided to base our investigation on simple and representative electron-rich and electron-poor aromatic and heteroaromatic substituents: (a) Pyridine (in **1a** and **1b**) as the representative standard of electron-poor heteroaromatic rings; (b) thiophene rings bearing either alkyl or primary electron-withdrawing functionalities (in **1c** and **1d**) as representative examples of donor and acceptor thiophene-based substituents, respectively; (c) benzene derivatives bearing electron-withdrawing (in **1e** and **1f**) and electron-donating (in **1g**) groups. Generally, alkyl chains have been introduced in some of the investigated derivatives also in order to improve their solubility in organic solvents in view of their potential use as DSSC electrolyte components. Indeed, it is commonly known that the presence of peripheral alkyl functionalities improves solubility of molecules in organic solvents [35–38] and reduces detrimental recombination phenomena [39,40].

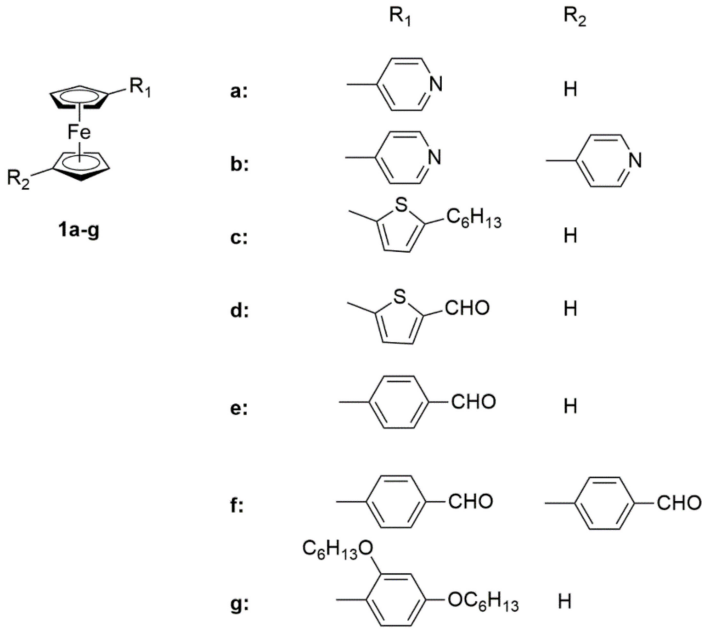

Figure 1. Mono- and bis-substituted Fc derivatives (**1a–g**).

Compounds **1a**, **1b**, and **1d–1f** were previously reported [41–45]. The synthetic scheme for the Fc derivatives **1c–1e** and **1g** is described in Scheme 1. The general procedure is a modification of the route previously reported by McGlinchey et al. used for the synthesis of anthracenylferrocene [46]. This synthetic scheme possesses wide applicability and can be easily extended to other derivatives pertaining to this class. The Fc derivatives have been synthesized via a Suzuki cross-coupling reaction starting from the proper ferroceneboronic acid except in the case of the products **1a, 1b**, and **1f**, where the corresponding pinacol ester was used (Scheme 2). The reaction with the corresponding arylbromide in presence of a Pd catalyst and an aqueous solution of tetrabutylammonium hydroxide as a base afforded the desired products. The ferrocenes derivatives **1a** and **1b** have been prepared in a single reaction starting from the 1,1′-ferrocenediboronic acid bis(pinacol) ester and obtained as pure products after column chromatography. The synthesis of **1f** is different from the one reported in literature. In fact, the exploited synthetic pathway allowed to achieve **1f** with 20% of yield in a single step, instead of an overall yield of 9% through three different steps previously reported [45].

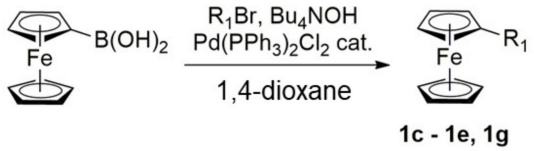

Scheme 1. Synthesis of compounds **1c–1e** and **1g** (R_1 as in Figure 1).

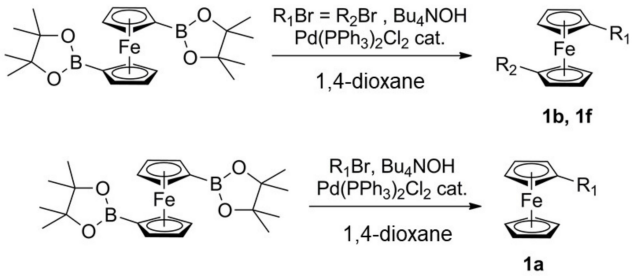

Scheme 2. Synthesis of compounds **1a,1b**, and **1f** (R_1 and R_2 as in Figure 1).

3.2. Optical Properties of Substituted Ferrocenes

The optical properties of the synthesized Fc derivatives in EtOH, for a direct comparison with the values reported in literature for iodide/triiodide, are shown in Figure 2. All the investigated compound showed an absorption peak in the range 447–484 nm with a molar extinction coefficient (ε) greater than 1000 M^{-1} cm^{-1} only for the formyl derivatives **1d–1f**. In the other cases, the value of ε is always lower than 800 M^{-1} cm^{-1} in the Vis range.

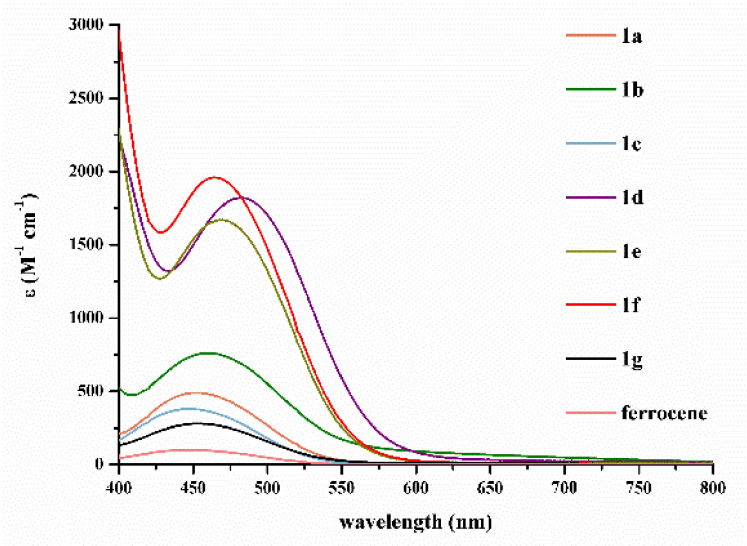

Figure 2. Absorption spectra of ferrocene-based compounds **1a–g** in EtOH.

We have analyzed the effect of the substituents on the Vis absorption band, that is of high impact in the implementation of a DSSC device using Fc/Fc^+ as a redox shuttle. Compared to the absorption band of the pristine Fc [47], the presence of substituents on the cyclopentadienyl ring shifts the absorption maximum to lower energies and this may be due to the extension of the π band. The presence of electron-poor substituents (**1a, 1b**, and **1d–1f**) induced a larger red-shift of the absorption peak, because of the more polarized structure, and also, in the case of the three formyl derivatives **1d–1f**, which have higher electron-withdrawing properties, a significant increase of the value of ε was observed (Table 1). Also, the compounds with the pyridine substituents presented a higher value of ε with respect to Fc, but it was of the same order of magnitude since the pyridine has a lower electron-withdrawing strength. The much lower absorption intensity in the Vis region of the new

Fc derivatives compared to the iodide/triiodide electrolyte, the ε value of which is 26,400 M^{-1} cm^{-1} at 353 nm [48,49], represents an important feature to be exploited in the photovoltaic device since competitive detrimental light absorption by the electrolyte is thus minimized and the solar spectrum might become more available for absorption by the photoactive anode.

Table 1. Absorption maxima and molar extinction coefficient of Fc-based derivatives **1a–1g** (EtOH).

Compound	λ_{max} (nm)	ε (M^{-1} cm^{-1})
iodide/triiodide [1]	353	26,400
Fc [2]	440	100
1a	452	490 ± 5
1b	460	760 ± 20
1c	447	380 ± 10
1d	484	1820 ± 80
1e	470	1670 ± 100
1f	464	1960 ± 100
1g	447	280 ± 10

[1] Values from Ref. [48]. [2] Values from Ref. [50].

3.3. Electrochemical Properties of Substituted Ferrocenes

Cyclic voltammetry (CV) was performed on derivatives **1a–1g** to determine the redox characteristics and HOMO/LUMO energy levels (Figure 3). The measured redox potentials, the HOMO/LUMO, and band gap energies are collected in Table 2 and pictorially summarized in Figure 4.

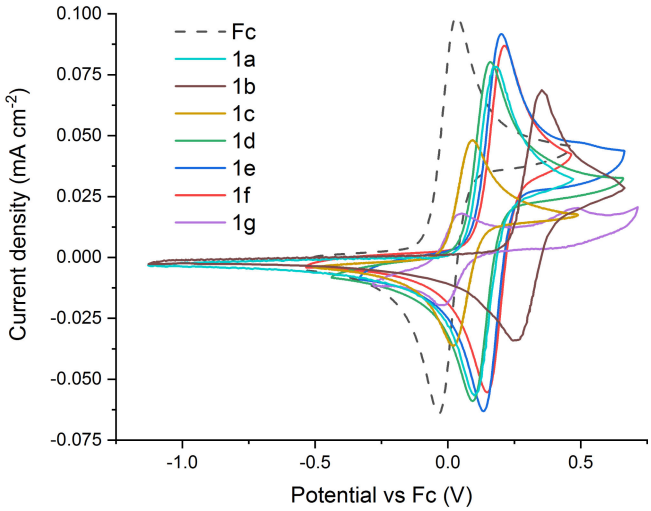

Figure 3. Cyclic voltammograms of compounds **1a–1g** (solid lines) and ferrocene as reference (dashed line) in 0.1 M $TBAClO_4$ in MeCN at a scan rate of 100 mV s^{-1}. The working, counter, and the pseudo-reference electrodes were a gold pin, a Pt wire, and an Ag/AgCl electrode (3 M KCl), respectively.

The energies of HOMO levels were calculated using the electrochemical oxidation potential (E_{ox}). LUMO levels were calculated using the HOMO energies and the values of the optical bandgaps, as estimated by means of Tauc plots [51]. The substituted Fc showed oxidation peaks at higher potentials compared to the bare Fc. Compounds bearing electron-rich groups (**1c**,**1g**) show similar oxidation potentials to Fc. In contrast, considering the results, the presence of electron-withdrawing substituents (**1a**,**1b** and **1d–1f**) afforded significantly more positive oxidation potentials, up to 0.35 eV, compared to Fc, thus validating the main scope of the work. It is worth noting from Figure 3 that, by designing a number of proper functionalized Fc substituents, a large variety of HOMO/LUMO energy levels can be

accessed, which is of primary importance for their use as electrolyte redox couples, in particular in DSSC devices with improved photovoltages.

Table 2. Electrochemical properties of Fc-based derivatives **1a–1g** (CH_3CN).

	E_{ox} vs. Fc (V)	E_{ox} vs. NHE [1] (V)	HOMO [2] (eV)	E_{gap}^{opt} (eV)	LUMO (eV)
Fc/Fc^+	0.00	0.63	−5.23	2.31	−2.92
1a	0.18	0.81	−5.41	2.30	−3.11
1b	0.35	0.98	−5.58	2.21	−3.37
1c	0.09	0.72	−5.32	2.34	−2.98
1d	0.13	0.76	−5.36	2.16	−3.20
1e	0.17	0.80	−5.40	2.18	−3.22
1f	0.18	0.81	−5.41	2.18	−3.23
1g	0.02	0.65	−5.25	2.33	−2.92

[1] All values have been calculated with Fc vs. NHE = 0.63 V in CH_3CN $TBAClO_4$ 0.1 M [Ref. [52]]. [2] Using a potential value of 4.60 eV for NHE vs. vacuum [Ref. [53]].

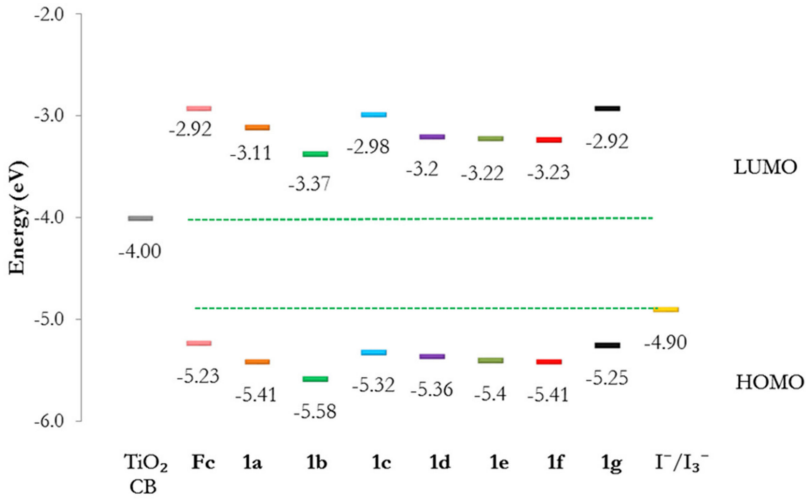

Figure 4. Scheme of the energy levels of the investigated Fc derivatives compared to the conduction band (CB) of TiO_2 and iodide/triiodide redox potential.

3.4. Spectroelectrochemistry

A strategic feature of a redox couple to be employed in DSSC is represented by the optical properties of its reduced and oxidized form. To properly investigate this feature, we decided to investigate the spectroelectrochemical behavior of the compounds **1a–1g** in the range 400–800 nm. Figure 5 depicts the UV-Vis spectra of the substituted Fc after electrochemical oxidation. Compounds with electron withdrawing substituents (**1a**,**1b** and **1d–1f**) exhibit an absorption band around 700 nm where most of the common sensitizers do not present any absorption band. The band of bis-substituted compounds (**1b**,**1f**) is red-shifted with respect to the corresponding mono-substituted compounds (**1a**,**1e**). The band of the Fc^+ derivatives with electron-donor substituents (**1c**,**1g**) was not visible in the recorded spectroelectrochemical spectra since the measurable spectral range was limited to 800 nm. The molar absorptivities of the oxidized forms (Fc^+) can be estimated by comparing the spectrum intensity with that of its corresponding reduced form (Fc). In particular, all of the oxidized compounds showed the main Vis band peak at wavelengths > 700 nm with an absorption intensity lower than that of the main band of the reduced forms.

As a further assessment of the reversibility of the oxidation process, an optical analysis has been carried out before the oxidation and after the reduction of the oxidized species (Figures S2–S8 in the Supplementary Data). We found that the redox process is reversible in all the investigated compounds,

because the reduction process of the oxidized compounds was able to successfully regenerate the original Fc derivatives as demonstrated from cyclic voltammetry (Figure 3) and spectroelectrochemistry. The reversibility of oxidation-reduction process is a key factor for the stability of DSSC devices.

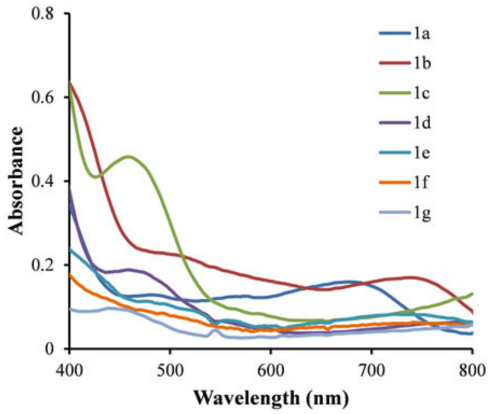

Figure 5. UV-Vis spectra of the compounds **1a–1g** after electrochemical oxidation.

4. Conclusions

A representative series of Fc derivatives, where the main core is substituted by one or two (located on different cyclopentadienyl rings) aromatic and heteroaromatic electron-donor and electron-acceptor substituents, has been designed, synthesized, and investigated for their optical and electrochemical properties. The general synthetic pathway is of wide pertinence and could be conveniently applied to the preparation of other interesting examples starting from readily available precursors. By adding the proper substituents, we were able to finely tune the optical and electrochemical properties and successfully access a large variety of HOMO/LUMO energies to be properly exploited in Fc-based electrolytes in solar devices. In particular, the electrochemical investigation showed that the presence of proper substituents is able to shift the redox potential to values up to ~0.4 V compared to Fc/Fc^+ and, more importantly, up to ~0.6 V compared to the iodide/triiodide couple. Thus, in principle, the maximum attainable photovoltage of a DSSC cell containing **1b/1b$^+$** as a redox couple can be increased of a remarkable value of 0.6 V. Interestingly, the absorption intensity of all of the new Fc derivatives, both in their reduced and oxidized form, is remarkably lower than those of the iodide/triiodide couple, which is remarkable in order to minimize detrimental competitive sunlight absorption with the photoactive dye-sensitized anode. Summarizing, the investigation of the substituted Fc derivatives might play a strategic role in the developments of new highly efficient, non-toxic, and cheap redox shuttle based on earth-abundant elements to be employed in solar devices as well as emerging energy technologies such as organic redox flow batteries.

Supplementary Materials: The following are available online at http://www.mdpi.com/1996-1073/13/15/3937/s1. The Supplementary materials contain the spectroelectrochemical studies, schematic electrochemical setup, ^{1}H-, ^{13}C-NMR, and HRMS spectra of the investigated compounds.

Author Contributions: The authors confirm their contribution to the work carried out in the field of: N.M.: writing—original draft, visualization, supervision, writing—review and editing; C.D.: investigation, writing—original draft; C.L.B.: visualization, writing—original draft; C.C.: investigation, data curation, methodology; A.A.: conceptualization, project administration, funding acquisition, writing—review and editing. All authors have read and agreed to the published version of the manuscript.

Funding: This research was funded by MIUR, grant Dipartimenti di Eccellenza—2017 "Materials for Energy," the national PRIN project "Unlocking Sustainable Technologies Through Nature-inspired Solvents" (NATUREChem) (grant number: 2017A5HXFC_002) and by University of Milano-Bicocca, grant Fondo di Ateneo-Quota Competitiva 2017 and 2019.

Acknowledgments: The authors acknowledge University of Milano-Bicocca for financial support.

Conflicts of Interest: The authors declare no conflict of interest. The funders had no role in the design of the study; in the collection, analyses, or interpretation of data; in the writing of the manuscript, or in the decision to publish the results.

References

1. O'Regan, B.; Grätzel, M. A low-cost, high-efficiency solar cell based on dye-sensitized colloidal TiO_2 films. *Nature* **1991**, *353*, 737–740. [CrossRef]
2. Abbotto, A.; Manfredi, N.; Manfredi, N. Electron-Rich heteroaromatic conjugated polypyridine ruthenium sensitizers for dye-sensitized solar cells. *Dalton Trans.* **2011**, *40*, 12421. [CrossRef] [PubMed]
3. Abbotto, A.; Manfredi, N.; Marinzi, C.; De Angelis, F.; Mosconi, E.; Yum, J.-H.; Xianxi, Z.; Nazeeruddin, M.K.; Grätzel, M. Di-Branched di-anchoring organic dyes for dye-sensitized solar cells. *Energy Environ. Sci.* **2009**, *2*, 1094–1101. [CrossRef]
4. Chen, C.; Liao, J.-Y.; Chi, Z.; Xu, B.; Zhang, X.; Kuang, D.-B.; Zhang, Y.; Liu, S.; Xu, J. Metal-Free organic dyes derived from triphenylethylene for dye-sensitized solar cells: Tuning of the performance by phenothiazine and carbazole. *J. Mater. Chem.* **2012**, *22*, 8994–9005. [CrossRef]
5. Wei, M.; Konishi, Y.; Zhou, H.; Yanagida, M.; Sugihara, H.; Arakawa, H. Highly efficient dye-sensitized solar cells composed of mesoporous titanium dioxide. *J. Mater. Chem.* **2006**, *16*, 1287–1293. [CrossRef]
6. Yella, A.; Lee, H.-W.; Tsao, H.N.; Yi, C.; Chandiran, A.K.; Nazeeruddin, K.; Diau, E.W.-G.; Yeh, C.-Y.; Zakeeruddin, S.M.; Grätzel, M. Porphyrin-Sensitized Solar Cells with Cobalt (II/III)-Based Redox Electrolyte Exceed 12 Percent Efficiency. *Science* **2011**, *334*, 629–634. [CrossRef]
7. Kakiage, K.; Aoyama, Y.; Yano, T.; Oya, K.; Fujisawa, J.-I.; Hanaya, M. Highly-Efficient dye-sensitized solar cells with collaborative sensitization by silyl-anchor and carboxy-anchor dyes. *Chem. Commun.* **2015**, *51*, 15894–15897. [CrossRef]
8. Zhang, S.; Yang, X.; Numata, Y.; Han, L. Highly efficient dye-sensitized solar cells: Progress and future challenges. *Energy Environ. Sci.* **2013**, *6*, 1443. [CrossRef]
9. Nazeeruddin, M.K.; De Angelis, F.; Fantacci, S.; Selloni, A.; Viscardi, G.; Liska, P.; Ito, S.; Takeru, A.B.; Grätzel, M. Combined Experimental and DFT-TDDFT Computational Study of Photoelectrochemical Cell Ruthenium Sensitizers. *J. Am. Chem. Soc.* **2005**, *127*, 16835–16847. [CrossRef]
10. Daeneke, T.; Kwon, T.-H.; Holmes, A.B.; Duffy, N.W.; Bach, U.; Spiccia, L. High-Efficiency dye-sensitized solar cells with ferrocene-based electrolytes. *Nat. Chem.* **2011**, *3*, 211–215. [CrossRef]
11. Daeneke, T.; Mozer, A.J.; Uemura, Y.; Makuta, S.; Fekete, M.; Tachibana, Y.; Koumura, N.; Bach, U.; Spiccia, L. Dye Regeneration Kinetics in Dye-Sensitized Solar Cells. *J. Am. Chem. Soc.* **2012**, *134*, 16925–16928. [CrossRef] [PubMed]
12. Sapp, S.A.; Elliott, C.M.; Contado, C.; Caramori, S.; Bignozzi, C.A. Substituted Polypyridine Complexes of Cobalt(II/III) as Efficient Electron-Transfer Mediators in Dye-Sensitized Solar Cells. *J. Am. Chem. Soc.* **2002**, *124*, 11215–11222. [CrossRef] [PubMed]
13. Wu, J.; Lan, Z.; Lin, J.; Huang, M.; Huang, Y.; Fan, L.; Luo, G. Electrolytes in Dye-Sensitized Solar Cells. *Chem. Rev.* **2015**, *115*, 2136–2173. [CrossRef]
14. Yanagida, S.; Yu, Y.; Manseki, K. Iodine/Iodide-Free Dye-Sensitized Solar Cells. *Acc. Chem. Res.* **2009**, *42*, 1827–1838. [CrossRef] [PubMed]
15. Cong, J.; Yang, X.; Kloo, L.; Sun, L. Iodine/iodide-free redox shuttles for liquid electrolyte-based dye-sensitized solar cells. *Energy Environ. Sci.* **2012**, *5*, 9180. [CrossRef]
16. Tian, H.; Sun, L. Iodine-Free redox couples for dye-sensitized solar cells. *J. Mater. Chem.* **2011**, *21*, 10592. [CrossRef]
17. Sun, Z.; Liang, M.; Chen, J. Kinetics of Iodine-Free Redox Shuttles in Dye-Sensitized Solar Cells: Interfacial Recombination and Dye Regeneration. *Accounts Chem. Res.* **2015**, *48*, 1541–1550. [CrossRef]
18. Colombo, A.; Di Carlo, G.; Dragonetti, C.; Magni, M.; Biroli, A.O.; Pizzotti, M.; Roberto, D.; Tessore, F.; Benazzi, E.; Bignozzi, C.A.; et al. Coupling of Zinc Porphyrin Dyes and Copper Electrolytes: A Springboard for Novel Sustainable Dye-Sensitized Solar Cells. *Inorg. Chem.* **2017**, *56*, 14189–14197. [CrossRef]
19. Hamann, T.W. The end of iodide? Cobalt complex redox shuttles in DSSCs. *Dalton Trans.* **2012**, *41*, 3111. [CrossRef]

20. Feldt, S.M.; Gibson, E.A.; Gabrielsson, E.; Sun, L.; Boschloo, G.; Hagfeldt, A. Design of Organic Dyes and Cobalt Polypyridine Redox Mediators for High-Efficiency Dye-Sensitized Solar Cells. *J. Am. Chem. Soc.* **2010**, *132*, 16714–16724. [CrossRef]
21. Kashif, M.K.; Axelson, J.C.; Duffy, N.W.; Forsyth, C.M.; Chang, C.J.; Long, J.R.; Spiccia, L.; Bach, U. A New Direction in Dye-Sensitized Solar Cells Redox Mediator Development: In Situ Fine-Tuning of the Cobalt(II)/(III) Redox Potential through Lewis Base Interactions. *J. Am. Chem. Soc.* **2012**, *134*, 16646–16653. [CrossRef] [PubMed]
22. Mosconi, E.; Yum, J.-H.; Kessler, F.; García, C.J.G.; Zuccaccia, C.; Cinti, A.; Nazeeruddin, M.K.; Grätzel, M.; De Angelis, F. Cobalt Electrolyte/Dye Interactions in Dye-Sensitized Solar Cells: A Combined Computational and Experimental Study. *J. Am. Chem. Soc.* **2012**, *134*, 19438–19453. [CrossRef] [PubMed]
23. Yum, J.-H.; Baranoff, E.; Kessler, F.; Moehl, T.; Ahmad, S.; Bessho, T.; Marchioro, A.; Ghadiri, E.; Moser, J.-E.; Yi, C.; et al. A cobalt complex redox shuttle for dye-sensitized solar cells with high open-circuit potentials. *Nat. Commun.* **2012**, *3*, 631. [CrossRef] [PubMed]
24. Chen, K.Y.; Du, C.; Patrick, B.O.; Berlinguette, C.P. High-Voltage Dye-Sensitized Solar Cells Mediated by [Co(2,2′-bipyrimidine)3]z. *Inorg. Chem.* **2017**, *56*, 2383–2386. [CrossRef]
25. Hao, Y.; Liang, M.; Wang, Z.; Wang, L.; Sun, Y.; Sun, Z.; Xue, S. 3,4-ethylenedioxythiophene as an electron donor to construct arylamine sensitizers for highly efficient iodine-free dye-sensitized solar cells. *Phys. Chem. Chem. Phys.* **2013**, *15*, 15441. [CrossRef]
26. Wang, Z.; Wang, H.; Liang, M.; Tan, Y.; Cheng, F.; Sun, Z.; Song, X. Judicious Design of Indoline Chromophores for High-Efficiency Iodine-Free Dye-Sensitized Solar Cells. *ACS Appl. Mater. Interfaces* **2014**, *6*, 5768–5778. [CrossRef]
27. Wang, Z.; Liang, M.; Wang, L.; Hao, Y.; Wang, C.; Sun, Z.; Xue, S. New triphenylamine organic dyes containing dithieno[3,2-b:2′,3′-d]pyrrole (DTP) units for iodine-free dye-sensitized solar cells. *Chem. Commun.* **2013**, *49*, 5748–5750. [CrossRef]
28. Tsao, H.N.; Yi, C.; Moehl, T.; Yum, J.-H.; Zakeeruddin, S.M.; Nazeeruddin, M.K.; Grätzel, M. Cyclopentadithiophene Bridged Donor-Acceptor Dyes Achieve High Power Conversion Efficiencies in Dye-Sensitized Solar Cells Based on the tris-Cobalt Bipyridine Redox Couple. *ChemSusChem* **2011**, *4*, 591–594. [CrossRef]
29. Perera, I.R.; Gupta, A.; Xiang, W.; Daeneke, T.; Bach, U.; Evans, R.; Ohlin, C.A.; Spiccia, L. Introducing manganese complexes as redox mediators for dye-sensitized solar cells. *Phys. Chem. Chem. Phys.* **2014**, *16*, 12021. [CrossRef]
30. Daeneke, T.; Mozer, A.J.; Kwon, T.-H.; Duffy, N.W.; Holmes, A.B.; Bach, U.; Spiccia, L. Dye regeneration and charge recombination in dye-sensitized solar cells with ferrocene derivatives as redox mediators. *Energy Environ. Sci.* **2012**, *5*, 7090. [CrossRef]
31. Hamann, T.W.; Farha, O.K.; Hupp, J.T. Outer-Sphere Redox Couples as Shuttles in Dye-Sensitized Solar Cells. Performance Enhancement Based on Photoelectrode Modification via Atomic Layer Deposition. *J. Phys. Chem. C* **2008**, *112*, 19756–19764. [CrossRef]
32. Daeneke, T.; Graf, K.; Watkins, S.; Thelakkat, M.; Bach, U. Infrared Sensitizers in Titania-Based Dye-Sensitized Solar Cells using a Dimethylferrocene Electrolyte. *ChemSusChem* **2013**, *6*, 2056–2060. [CrossRef] [PubMed]
33. Perera, I.R.; Daeneke, T.; Makuta, S.; Yu, Z.; Tachibana, Y.; Mishra, A.; Bäuerle, P.; Ohlin, C.A.; Bach, U.; Spiccia, L. Application of the Tris(acetylacetonato)iron(III)/(II) Redox Couple in p-Type Dye-Sensitized Solar Cells. *Angew. Chem. Int. Ed.* **2015**, *54*, 3758–3762. [CrossRef] [PubMed]
34. Yum, J.-H.; Holcombe, T.; Kim, Y.; Yoon, J.; Rakstys, K.; Nazeeruddin, M.K.; Grätzel, M. Towards high-performance DPP-based sensitizers for DSC applications. *Chem. Commun.* **2012**, *48*, 10727–10729. [CrossRef] [PubMed]
35. Khalid, H.; Wang, L.; Yu, H.; Akram, M.; Abbasi, N.M.; Sun, R.; Saleem, M.; Abdin, Z.U.; Chen, Y. Synthesis of Soluble Ferrocene-Based Polythiophenes and Their Properties. *J. Inorg. Organomet. Polym. Mater.* **2015**, *25*, 1511–1520. [CrossRef]
36. Tajima, K.; Huxur, T.; Imai, Y.; Motoyama, I.; Nakamura, A.; Koshinuma, M. Surface activities of ferrocene surfactants. *Colloids Surf. A Physicochem. Eng. Asp.* **1995**, *94*, 243–251. [CrossRef]
37. Forster, S.; Buckton, G.; Beezer, A.E. The importance of chain length on the wettability and solubility of organic homologs. *Int. J. Pharm.* **1991**, *72*, 29–34. [CrossRef]

38. Wei, X.; Cosimbescu, L.; Xu, W.; Hu, J.Z.; Vijayakumar, M.; Feng, J.; Hu, M.Y.; Deng, X.; Xiao, J.; Liu, J.; et al. Batteries: Towards High-Performance Nonaqueous Redox Flow Electrolyte Via Ionic Modification of Active Species. *Adv. Energy Mater.* **2015**, *5*, 1400678. [CrossRef]
39. Hagfeldt, A.; Boschloo, G.; Sun, L.; Kloo, L.; Pettersson, H. Dye-Sensitized Solar Cells. *Chem. Rev.* **2010**, *110*, 6595–6663. [CrossRef]
40. Hamann, T.W.; Ondersma, J.W. Dye-Sensitized solar cellredox shuttles. *Energy Environ. Sci.* **2011**, *4*, 370–381. [CrossRef]
41. Miller, T.M.; Ahmed, K.J.; Wrighton, M.S. Complexes of rhenium carbonyl containing ferrocenyl-derived ligands: Tunable electron density at rhenium by control of the redox state of the ferrocenyl ligand. *Inorg. Chem.* **1989**, *28*, 2347–2355. [CrossRef]
42. Braga, D.; D'Addari, D.; Polito, M.; Grepioni, F. Mechanically Induced Expeditious and Selective Preparation of Disubstituted Pyridine/Pyrimidine Ferrocenyl Complexes. *Organometallics* **2004**, *23*, 2810–2812. [CrossRef]
43. Imrie, C.; Loubser, C.; Engelbrecht, P.; McCleland, C.W. The use of a modified Suzuki reaction for the synthesis of monoarylferrocenes. *J. Chem. Soc. Perkin Trans. 1* **1999**, *17*, 2513–2523. [CrossRef]
44. Plyta, Z.F.; Prim, D.; Tranchier, J.-P.; Rose-Munch, F.; Rose, E. Tricarbonyl(η6-arene)chromium and ferrocene complexes linked with aromatic spacers. *Tetrahedron Lett.* **1999**, *40*, 6769–6771. [CrossRef]
45. Shimizu, I.; Umezawa, H.; Kanno, T.; Izumi, T.; Kasahara, A. Synthesis of [0]Orthocyclo[2]orthocyclo[0](1,1′)ferrocenophane and [0]Paracyclo[0](1,1′)ferrocenophane. *Bull. Chem. Soc. Jpn.* **1983**, *56*, 2023–2028. [CrossRef]
46. Nikitin, K.; Müller-Bunz, H.; Ortin, Y.; Muldoon, J.; McGlinchey, M.J. Molecular Dials: Hindered Rotations in Mono- and Diferrocenyl Anthracenes and Triptycenes. *J. Am. Chem. Soc.* **2010**, *132*, 17617–17622. [CrossRef]
47. Li, D.; Zhang, Y.; Jiang, J.; Li, J. Electroactive gold nanoparticles protected by 4-ferrocene thiophenol monolayer. *J. Colloid Interface Sci.* **2003**, *264*, 109–113. [CrossRef]
48. Awtrey, A.D.; Connick, R.E. The Absorption Spectra of I_2, I_3^-, I^-, IO_3^-, S_4O_6= and S_2O_3=. Heat of the Reaction $I_3^- = I_2 + I^-$. *J. Am. Chem. Soc.* **1951**, *73*, 1842–1843. [CrossRef]
49. Boschloo, G.; Hagfeldt, A. Characteristics of the Iodide/Triiodide Redox Mediator in Dye-Sensitized Solar Cells. *Acc. Chem. Res.* **2009**, *42*, 1819–1826. [CrossRef]
50. Sarhan, A.A.O.; Ibrahim, M.S.; Kamal, M.M.; Mitobe, K.; Izumi, T. Synthesis, cyclic voltammetry, and UV–Vis studies of ferrocene-dithiafulvalenes as anticipated electron-donor materials. *Mon. Chem. Chem. Mon.* **2008**, *140*, 315–323. [CrossRef]
51. Tauc, J. Optical properties and electronic structure of amorphous Ge and Si. *Mater. Res. Bull.* **1968**, *3*, 37–46. [CrossRef]
52. Pavlishchuk, V.V.; Addison, A.W. Conversion constants for redox potentials measured versus different reference electrodes in acetonitrile solutions at 25 °C. *Inorgan. Chim. Acta* **2000**, *298*, 97–102. [CrossRef]
53. Bockris, J.O.M.; Khan, S.U.M. *Surface Electrochemistry—A Molecular Level Approach*; Springer: New York, NY, USA, 1993.